Bull. Mater. Sci., Vol. 37, No. 3, May 2014, pp. 655–660. © Indian Academy of Sciences.

Hydrogen absorption/desorption characteristics of room temperature $ZrMn_{2-x}Ni_x$ system (x = 1·25–1·50)

VINOD KUMAR[a], D PUKAZHSELVAN[a,b], A K TYAGI[c] and S K SINGH[a,*]

[a]Department of Physics, Deenbandhu Chhotu Ram University of Science and Technology, Murthal 131 039, India

[b]Department of Physics, Padova University, Padova, Italy

[c]Solid State Chemistry Section, Babha Atomic Research Centre, Mumbai 400 085, India

MS received 5 December 2012; revised 27 February 2013

Abstract. **The present communication deals with the hydrogen storage characteristics of C15 laves phase $ZrMn_{2-x}Ni_x$ system tailored within the x values of 1·25 to 1·50. Drastic variations in thermodynamics of the hydride phase is observed for any little changes of concentration x within this narrow range. The most promising room temperature hydrogen storage materials are found to be formed within the range of 1·35 to 1·45 where ~ 2·5 to 2·9 H/F.U. can be reversibly stored under the ideal operating conditions. The heat of the reaction is found to be ~ 17 kJ/mol, which means these are promising candidates for stationary and short range mobile applications. The phase structural features and the thermodynamic aspects of all the materials are discussed in detail.**

Keywords. **$ZrMn_{2-x}Ni_x$ system; metal hydrides; hydrogen storage materials.**

1. Introduction

Metal hydrides are the most attractive means of hydrogen storage system for vehicular applications. As per the USDOE's referred technical target, for the success of hydrogen economy, it is essential to develop a hydrogen storage material which can reversibly store ~5·5 wt.% of hydrogen under ideal operating conditions (Satyapal *et al* 2007; Yang *et al* 2010). In spite of extensive investigations on a wide variety of metal hydride systems, it is not yet possible to reach this hallmark without compromising the performance requirements. As for example, the promising light weight hydrides such as $NaAlH_4$ (5·5 wt.%) and MgH_2 (7·6 wt.%) systems are operative only above the range of 150 to 350 °C (Bogdanovic *et al* 2000; Hanada *et al* 2005; Pukazhselvan *et al* 2012). To date, the best hydrogen storage materials, from performance point of view, are intermetallic hydrides (Mani and Ramaprabhu 2004; Kandavel and Ramaprabhu 2004). The storage capacity of most of the intermetallic hydrides hangs around 1 wt.% which is clearly not sufficient for vehicular applications. However, it is logical to assume that any high performance STP system with ~ 1·5 wt.% reversible capacity can be competitive for short range vehicular applications. Additionally, such hydrides are very useful for stationary applications, such as hydrogen filling stations, large scale storage cylinders in hydrogen production spots, electrochemical devices, etc (Rodrigues *et al* 2000, Pukazhselvan *et al* 2012).

It is also important to consider that, if an intermetallic system stores ~ 1·5 wt.% hydrogen within few seconds and liberates it under ambient conditions, then it is possible to serve better the present day battery/fuel cell vehicles (using high pressure cylinders) for uninterrupted transport within 50 to 100 km. However, poor activation characteristics, poor stability and kinetic limitations are some of the important setbacks associated with most of the intermetallic systems known so far (Kumar *et al* 2012). Recent reports suggest that it is possible to improve the capacity and thermodynamic features of laves phase systems through appropriate material tailoring routes (Suda and Sandrock 1994; Okada *et al* 2002). In the present investigation, we propose the Zr based promising laves phase system $ZrMn_{2-x}Ni_x$, which absorbs and desorbs hydrogen within a few seconds under room temperature. Hong and Fu (2002) have previously investigated several Zr based AB_2 hydrides such as ZrV_2, $ZrCr_2$, $ZrMn_2$, $ZrFe_2$, $ZrCo_2$ and $ZrNi_2$, etc. It was shown that the absolute value of the hydrogen binding energy with the laves phase decreases as the atomic number of B site element increases. This trend suggests that $ZrCr_2$ and $ZrMn_2$ form the most stable hydrides and $ZrNi_2$ forms the least stable hydride. Thus, we expect interesting thermodynamic effects by mixing the Mn and Ni atoms for B sites in Zr based (i.e. Zr–Mn–Ni) laves phase. Additionally, the in-depth DFT calculations of Gesari *et al* (2010) suggests that the favourability of hydrogen occupation

*Author for correspondence (sksingh2k6@gmail.com)

goes in the sequence of A_2B_2, AB_3 and B_4 tetrahedral sites of the laves phases and the hydrogen occupation varies from high to low in the sequence of $A_2B_2 > AB_3 > B_4$. Moreover, the binding energy calculations reveal that the whichever tetrahedral sites are rich with 'A' atoms exhibits higher interaction energy than the sites with 'B' atoms. It is also known that the bonding of Ni–H is weaker than the bonding of both Zr–H and Mn–H. Therefore, it is reasonable to expect that some hydride compositions of $ZrMn_{2-x}Ni_x$ could possibly be not so stable like $ZrMn_2H_x$ and also not much unstable like $ZrNi_2H_x$.

In our previous work, we investigated the $ZrMn_{2-x}Ni_x$ system for the range of x values from 0 to 2 and identified that a narrow range of $x = 1{\cdot}25$ to $1{\cdot}50$ may possess considerable promise for reversible hydrogen storage applications. We noticed a dramatic difference between $ZrMn_{0{\cdot}50}Ni_{1{\cdot}50}$ and $ZrMn_{0{\cdot}75}Ni_{1{\cdot}25}$ in its interaction with hydrogen. Thus in the present work, we decided to tailor and characterize the materials with very small concentration changes with the step difference of 0·05. We observed that most promising hydrogen storage candidates of this class were formed within a narrow range where the concentration of Mn lay between 0·55 and 0·60. Hydrogen absorption/desorption can be achieved within 20 seconds which seems to be a significant result for applications. The crystal system of all the synthesized materials is observed to be C15 type cubic phase.

2. Experimental

All the required chemicals such as Zr, Ni and Mn, were procured from Alfa Aesar Chemicals Ltd. The compositions of $AB_{2-x}B'_x$ (B = Mn and B′ = Ni) were calculated as required for the powder mixer taken in right stoichiometry. For every composition, 5 g of materials were pelletized by 100 KN load (pellet thickness: 5 mm and diameter: 15 mm) and the pellets were melted under inert ambient using a high frequency induction furnace (20 kW, 12 kHz) supplied by Inductotherm India Pvt Ltd, Ahmedabad. For hydrogen absorption/desorption measurements, two grams of samples were loaded in a metal-hydrogen high pressure reaction chamber. The PCT absorption/desorption measurements have been performed by a digitalized Sievert's type apparatus attached with microprocessor controlled programmable furnace. Series of PCT isotherms have been recorded over a range of temperature between 0 and 120 °C and the enthalpy of desorption (ΔH) was calculated from the van't Hoff equation as given by:

$$\ln P_{eq} = -\frac{\Delta H}{RT} + \frac{\Delta S}{R},$$

where P_{eq} is the equilibrium plateau pressure, R the gas constant and T the reaction temperature. By plotting $1/T$ vs $\ln P_{eq}$, both the enthalpy of desorption (ΔH) and the entropy values (ΔS) can be calculated.

XRD analysis of all the samples were performed by Regaku mini Flex11 X-ray diffractometer employing CuKα radiation ($\lambda = 1{\cdot}541$ Å). The diffraction patterns were indexed by comparing the observed pattern with the standard JCPDF data source files. The lattice parameters were calculated using the simple unit cell refinement technique and the size of crystallites was calculated using Scherror method.

3. Results and discussion

In our previous work we investigated the $ZrMn_{2-x}Ni_x$ system over $x = 0$ to 2 with a step difference of 0·25. We noticed a significant difference in the hydrogen sorption performances between the compositions $ZrMn_{0{\cdot}50}Ni_{1{\cdot}50}$ and $ZrMn_{0{\cdot}75}Ni_{1{\cdot}25}$. The former composition absorbs and releases hydrogen under room temperature whereas the latter absorbs hydrogen at room temperature but releases hydrogen at above 100 °C. Noticeably, no significant interaction with hydrogen was observed within the Mn concentration of 0 to < 0·50 whereas very stable hydrides were formed within the range of > 0·75 to 2. It is, therefore, clear that the most promising hydrogen storage candidate of this class could be within the range of these two compositions $ZrMn_{0{\cdot}50}Ni_{1{\cdot}50}$ and $ZrMn_{0{\cdot}75}Ni_{1{\cdot}25}$. With this background, we have further investigated the effect of small variation of concentration (Mn and Ni with a step variation of 0·05) on the hydrogen storage performances of the system. The XRD picture of the as-prepared $ZrMn_{0{\cdot}50}Ni_{1{\cdot}50}$, $ZrMn_{0{\cdot}60}Ni_{1{\cdot}40}$, $ZrMn_{0{\cdot}75}Ni_{1{\cdot}25}$ and the hydrogen charged $ZrMn_{0{\cdot}60}Ni_{1{\cdot}40}$ are shown in figure 1. The XRDs illustrate that all these compositions possess cubic C15 type laves phases (Pearson's Crystal Data; Sun *et al* 2007) along with a smaller amount of Zr_7Ni_{10} alloy (Yang *et al* 2000; Young *et al* 2010). All the structural details of these samples are summarized in table 1. Careful analysis suggests that, when the system interacts with hydrogen, the microstructure of these systems gets affected (crystallite size gets reduced) but the lattice structure of the laves phase remains unaffected. The insertion of hydrogen in the laves phase leads to significant lattice expansion and, consequently, the microstructure of the system gets influenced. One can understand it from the difference of crystallite sizes before and after hydrogenation of the material. As for example, in the case of $ZrMn_{0{\cdot}60}Ni_{1{\cdot}40}$, the crystallite size of the as-received material is ~ 39 nm and this size gets reduced to ~ 26 nm by hydrogenation of the alloy (table 1). The expansion usually leads to deep cracks in the microstructure (Tsukahara *et al* 1996), so the hydrogenated material usually exhibits lower particle/crystallite size as compared to the neat as-prepared material.

Figure 2 shows hydrogen absorption kinetics (first exposure) curves of the alloys $ZrMn_{0{\cdot}50}Ni_{1{\cdot}50}$,

Table 1. Structural details of samples $ZrMn_{0.50}Ni_{1.50}$, $ZrMn_{0.60}Ni_{1.40}$, $ZrMn_{0.75}Ni_{1.25}$ and hydrided $ZrMn_{0.60}Ni_{1.40}$.

Sl. no.	Composition	Lattice parameter (Å)	Cell volume	Crystal size (nm)
1	$ZrMn_{0.50}Ni_{1.50}$ (C15)	7·021 ± 0·0016	345·92 ± 0·235	38·28
2	$ZrMn_{0·60}Ni_{1.40}$ (C15)	7·025 ± 0·0016	346·63 ± 0·236	39·0
3	$ZrMn_{0.75}Ni_{1.25}$ (C15)	7·037 ± 0·0048	348·53 ± 0·711	27·82
4	Hyd. $ZrMn_{0.60}Ni_{1.40}$ (C15)	7·023 ± 0·0010	346·43 ± 0·146	25·95

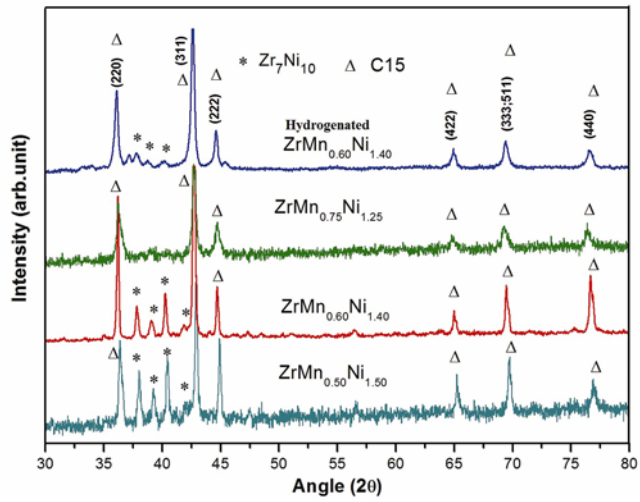

Figure 1. XRD patterns of samples C15 laves phase intermetallic systems such as $ZrMn_{0.50}Ni_{1.50}$, $ZrMn_{0.60}Ni_{1.40}$, $ZrMn_{0.75}Ni_{1.25}$ and hydrided $ZrMn_{0.60}Ni_{1.40}$.

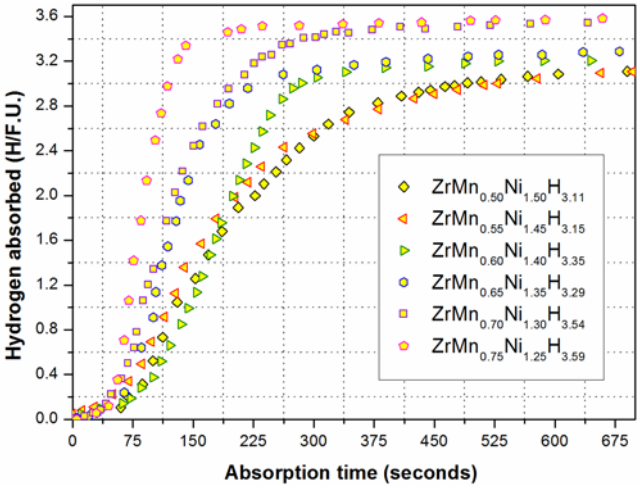

Figure 2. Hydrogen uptake kinetics recorded during first hydrogen exposure for as-prepared AB_2 systems such as $ZrMn_{0.50}Ni_{1.50}$, $ZrMn_{0.55}Ni_{1.45}$, $ZrMn_{0.60}Ni_{1.40}$, $ZrMn_{0.65}Ni_{1.35}$, $ZrMn_{0.70}Ni_{1.30}$ and $ZrMn_{0.75}Ni_{1.25}$.

$ZrMn_{0.55}Ni_{1.45}$, $ZrMn_{0.60}Ni_{1.40}$, $ZrMn_{0.65}Ni_{1.35}$, $ZrMn_{0.70}Ni_{1.30}$ and $ZrMn_{0.75}Ni_{1.25}$. As seen, $ZrMn_{0.50}Ni_{1.50}$ stores ~ 3·1 H/F.U. with appreciable kinetics. While we increase the Mn concentration from 0·50 to 0·75 with a step concentration of 0·05, the kinetics gradually improves and the storage capacity also sets to a maximum value of ~ 3·6 H/F.U. One of the major difficulties of laves phase hydrides is their higher stability and it is difficult to reversibly store the absorbed hydrogen under manageable operating conditions (Douglas *et al* 1996; Yang *et al* 1996). But the $ZrMn_{2-x}Ni_x$ group of materials within the Mn concentration range of 0·50 to 0·75 forms interesting hydrogen storage candidates due to the fact that a significant fraction of the absorbed hydrogen can be released under room temperature. As shown in figure 3, hydrogen liberation can be observed with very good kinetics in materials with Mn concentrations just above 0·50 and the kinetics is slow at the concentration closer to the values of 0·75. Thus, more interesting composition for desorption seems to be within the range of Mn values of 0·50 to 0·60. Further kinetic analysis over a wide range of temperatures revealed that the effective hydrogen storage capacity of these materials was within ~ 2·8 to 3 H/F.U. (A summary of data is shown in table 2). The reversible hydrogen absorption kinetics of all the dehydrogenated materials is shown in figure 4. The curves show that all the released hydrogen can be reversibly stored with faster absorption kinetics. Almost two-thirds capacity of the total effective capacity in each case can be restored within the first 20 s. Thus, these materials appear to be promising for a variety of stationary applications and also for a short range vehicular applications.

Apart from the kinetic consideration of any materials, yet another most important property is the thermodynamics. The reaction enthalpy values are required to be within the range of 14 to 24 kJ/mol for commercial applications (Pukazhselvan *et al* 2012). In order to explore the thermodynamics, we carried out the PCT absorption and desorption characteristics of $ZrMn_{2-x}Ni_x$ (x = 0·50, 0·55, 0·60, 0·65, 0·70 and 0·75). The PCT absorption isotherm for all these compositions is shown in figure 5. It is interesting to note that the variation of absorption plateau pressure is much higher for such a small variation of Mn concentration, i.e. 0·05. It clearly indicates that the thermodynamics of the $ZrMn_{2-x}Ni_x$ system is very sensitive to the concentration changes within the x values of 1·25 to 1·50. The PCT absorption isotherm reveals that the composition $ZrMn_{0.75}Ni_{1.25}$ can absorb hydrogen under near STP conditions with a much favourable equilibrium pressure. As we decrease the Mn concentration, the plateau

Table 2. Hydrogen absorption/desorption capacity and plateau pressure values obtained for all samples discussed in present study.

Sl. no.	Composition	Hydrogen capacity (H/F.U.)	Plateau pressure (atm)	
			Absorption at 30 °C	Desorption 60 °C
1	$ZrMn_{0.75}Ni_{1.25}$	3·59	4	
2	$ZrMn_{0.70}Ni_{1.30}$	3·54	15	3·5
3	$ZrMn_{0.65}Ni_{1.35}$	3·29	22·5	4·75
4	$ZrMn_{0.60}Ni_{1.40}$	3·35	31·5	6·5
5	$ZrMn_{0.55}Ni_{1.45}$	3·15	37·5	8
6	$ZrMn_{0.50}Ni_{1.50}$	3·11	41	9

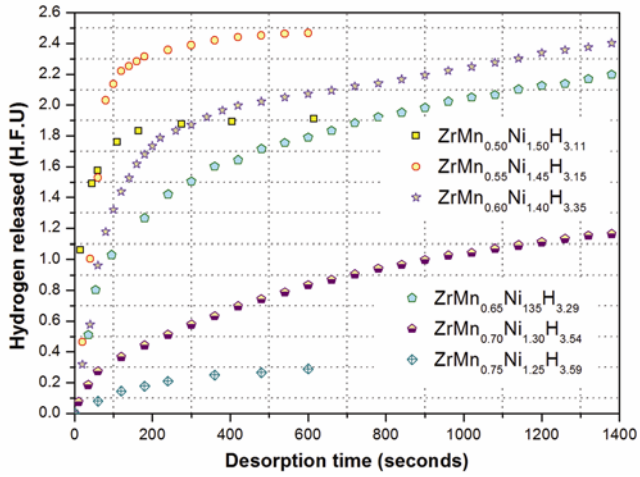

Figure 3. Dehydrogenation kinetics of all hydrogenated samples discussed in present study. Captions of individual samples are given in figure.

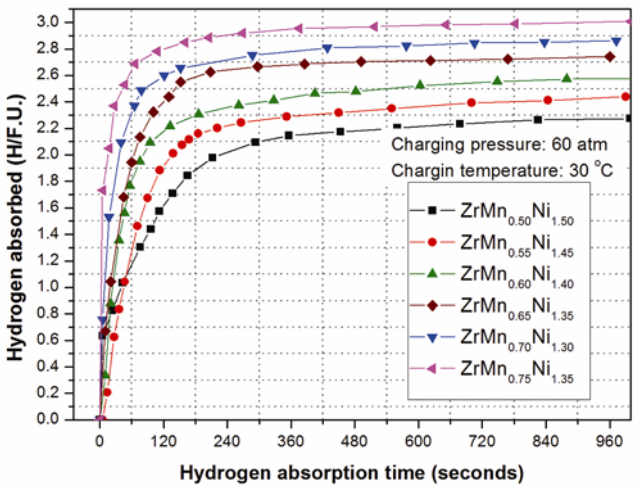

Figure 4. Reversible hydrogen absorption kinetics of all dehydrogenated samples. Note that obtained capacity values in this figure represent actual capacity limit (effective storage capacity) of these materials.

pressure rises up and goes in excess of 40 atm for the composition of $ZrMn_{0.50}Ni_{1.50}$ with decreasing trend in the uptake capacity. It indicates that the stability of the hydride phase decreases as we decrease the concentration of Mn. Both the higher and lower stabilities are not desirable for applications. Thus, it appears to be the mid values within the range of $x = 1.25$ to 1.50 that can be treated to be good for reversible hydrogen absorption, in this case. During desorption (figure 6), the plateau pressure of $ZrMn_{0.75}Ni_{1.25}$ drops lower than 1 atm at room temperature and better PCT desorption performances are observed in the case of all other compositions.

The data derived from a series of absorption and desorption PCT study are given in table 3. The van't Hoff plots, calculated from the PCT desorption curves for all the compositions discussed in the present study, are given in figure 7. The PCT curves provide a better picture regarding the equilibrium pressures and the corresponding desorption temperatures for all the compositions. As can be noticed, the thermodynamics varies considerably from the composition $ZrMn_{0.55}Ni_{1.45}$ and the materials are comparatively stable above the composition of $ZrMn_{0.70}Ni_{1.30}$. All the relevant thermodynamic data are summarized in table 3. The values suggest that the most feasible thermodynamics can be obtained in the composition of $ZrMn_{0.55}Ni_{1.45}$ and $ZrMn_{0.60}Ni_{1.40}$ and, from capacity and kinetics point of view, these two compositions seem to be very promising. Thus, starting from $ZrMn_{2-x}Ni_x$ for $x = 0$ to 2, we narrowed down to $x = 1.40$ to 1.45 which is the region for most promising Zr–Mn–Ni systems for applications.

In the case of intermetallic hydrides, the surface catalysts play a main role in breaking the hydrogen molecules into atoms for the formation of metal hydrides (for more insights into the metal-hydrogen interaction, the reader is referred to the recent review of Pukazhselvan *et al* (2012). However, as far as the stability of the laves phase hydrides are concerned, tailoring of the $A_2B_2/AB_3/B_4$ sites mainly determines the performance of the system. The detailed studies regarding the interaction between the laves phase and the hydrogen molecules have previously been explored by many theoretical investigators (Nagasako *et al* 2002; Herbst and Hector 2007; Al Alam *et al* 2008; Yartys *et al* 2008; Gesari *et al* 2010). Nagasako *et al* (2002) have shown that the heat of formation of the laves phase hydride exhibits a strong relation with the

Table 3. Thermodynamic parameters such as heat of reaction, entropy and equilibrium pressure observed by PCT measurements.

Sr. no.	Composition	ΔH (kJ/mol H)	ΔS (J/(K mol H))	Desorption temp. at equilibrium pressure of 1 atm (°C)
1	$ZrMn_{0.75}Ni_{1.25}$	27·97 ± 1·82	74·87 ± 4·32	100·01
2	$ZrMn_{0.70}Ni_{1.30}$	23·35 ± 0·86	77·92 ± 2·89	26·7
3	$ZrMn_{0.65}Ni_{1.35}$	19·56 ± 1·37	71·56 ± 4·27	0
4	$ZrMn_{0.60}Ni_{1.40}$	17·67 ± 0·05	67·92 ± 0·16	–12·85
5	$ZrMn_{0.55}Ni_{1.45}$	17·152 ± 0·47	68·87 ± 1·48	–22·18
6	$ZrMn_{0.50}Ni_{1.50}$	18·61 ± 1·14	73·74 ± 3·60	–20·10

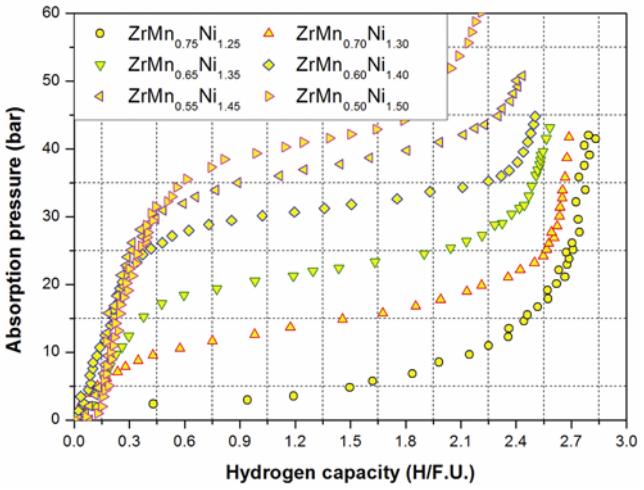

Figure 5. PCT absorption isotherms of all materials discussed in present study.

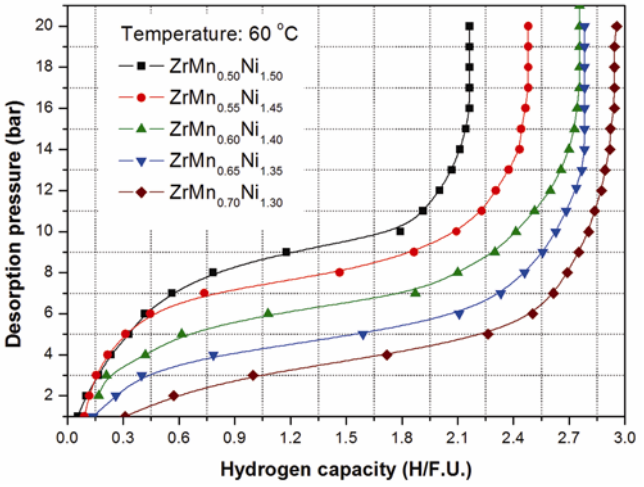

Figure 6. PCT desorption isotherms of all materials of present study.

energy values associated with volume expansion and the energy gain, as a result of the insertion of hydrogen in interstitials. It means, dopants like Ni can strongly influence the heat of reaction and also the interaction of laves phase with hydrogen. Additionally, it is also known that the presence of Zr_7Ni_{10} secondary phase is beneficial for

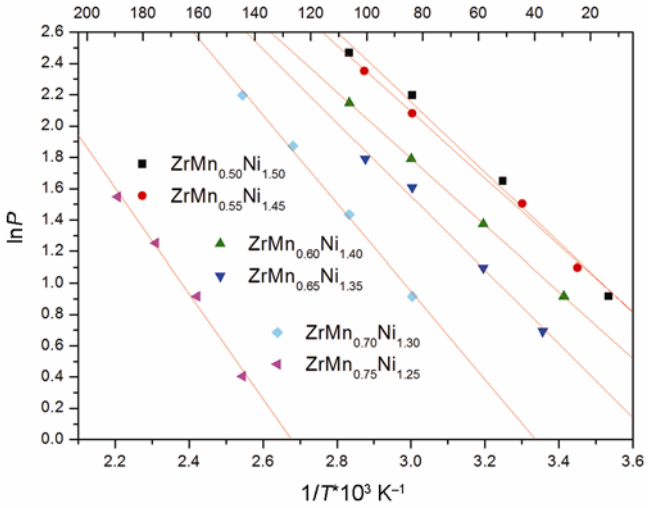

Figure 7. van't Hoff plots calculated from PCT desorption data. Equilibrium pressure at room temperature for all compositions are summarized in table 3.

offering higher catalytic activity. Thus, doping of Ni in $ZrMn_2$ parent alloy not only leads to excellent tuning of thermodynamics but also renders higher catalytic activity.

4. Conclusions

Thermodynamically promising $ZrMn_{2-x}Ni_x$ hydrogen storage materials can be tailored within the range of $x = 1{\cdot}25$ to $1{\cdot}50$. Any slight variation of x values within this region results in dramatic changes in the thermodynamics of the hydride. More careful analysis reveal that the compositions $ZrMn_{0{\cdot}55}Ni_{1{\cdot}45}$, $ZrMn_{0{\cdot}60}Ni_{1{\cdot}40}$, $ZrMn_{0{\cdot}65}Ni_{1{\cdot}35}$ are very promising hydrogen storage materials with the reaction enthalpy of ~ 17 to ~ 20 kJ/mol. Moreover, almost two-thirds of the effective hydrogen capacity (absorption and desorption) can be achieved within a few seconds. Thus these materials are competing candidates for both stationary applications and short range vehicular applications.

Acknowledgements

The authors thank Dr V C Shahni of BARC for discussions and Dr H K Singh and Dr D K Mishra of NPL for

providing XRD facility. (DP) thanks UGC, Government of India for D S Kothari Post-doctoral Fellowship and (VK) thanks the Department of Atomic Energy, Government of India, for a Senior Research Fellowship. This work has been carried out under the financial assistance provided by BRNS, Department of Atomic Energy, Government of India.

References

Al Alam A F, Matar S F, Ouïni N and Nakhl M 2008 *Prog. Solid State Chem.* **36** 192

Bogdanovic B, Brand R A, Marjanovic A, Schwickardi M and Tölle J 2000 *J. Alloys Compd.* **302** 36

Douglas G, Ivey, Derek O and Northwood 1996 *Z. Phys. Chem.* **147** 191

Gesari S B, Pronsato M E, Visintin A and Juan A 2010 *J. Phys. Chem.* **C114** 16832

Hanada N, Ichikawa T and Fujii H 2005 *J. Phys. Chem.* **B109** 7188

Herbst J F and Hector L G 2007 *J. Alloys Compd.* **446–447** 188

Hong S and Fu C L 2002 *Phys. Rev.* **B66** 094109

Kandavel M and Ramaprabhu S 2004 *J. Alloys Compd.* **381** 140

Kumar V, Pukazhselvan D and Singh S K 2012 *Adv. Sci. Lett.* **5** 1

Mani N and Ramaprabhu S 2004 *J. Alloys Compd.* **363** 275

Nagasako N, Fukumoto A and Miwa K 2002 *Phys. Rev.* **B66** 155106

Okada M, Kuriiwa T, Kamegawa A and Takamura H 2002 *Mater. Sci. Eng.* **A329–331** 305

Pearson's Crystal Data, Powder pattern of: 454298: Ni_2Zr – $MgCu_2$, cF24, 227, http://cst-www.nrl.navy.mil/lattice/struk/c15.html

Pukazhselvan D, Kumar V and Singh S K 2012 *Nano Energy* **1** 566

Pukazhselvan D, Saravanan R S S and Yadav T P 2012 *Rev. Adv. Sci. Eng.* **1** 302

Pukazhselvan D, Sterlin M S L and Srivastava O N 2012 *Int. J. Hydrogen Energy* **37** 3697

Pukazhselvan D 2012 *Int. J. Hydrogen Energy* **37** 9696

Rodrigues S, Munichandraiah N and Shukla A K 2000 *Bull. Mater. Sci.* **23** 383

Satyapal S, Petrovic J, Read C, Thomas G and Ordaz G 2007 *Catalysis Today* **120** 246

Suda S and Sandrock G 1994 *Z. Phys. Chem.* **183** 149

Sun J C, Li S and Ji S J 2007 *J. Alloys Compd.* **446–447** 630

Tsukahara M, Takahashi K, Mishima T, Isomura A and Sakai T 1996 *J. Alloys & Compd.* **236** 151

Yang J, Sudik A, Wolverton C and Siegel D J 2010 *Chem. Soc. Rev.* **39** 656

Yang J, Ciureanu M and Roberge R 2000 *Mater. Lett.* **43** 234

Yang X G, Lei Y Q, Zhang W K, Zhu G M and Wang Q D 1996 *J. Alloys Compd.* **243** 151

Yartys V A, Vajeeston P, Riabov A B, Ravindran P, Denys R V, Maehlen J P, Delaplane R G and Fjellvåg H Z 2008 *Kristallogr.* **223** 674

Young K, Ouchi T, Huang B, Chao B, Fetcenko M A, Bendersky L A, Wang K and Chiu C 2010 *J. Alloys Compd.* **506** 841